# RESEARCH IN SEISMOLOGY

Carl Kisslinger, et al

Saint Louis University

Prepared for:

Air Force Cambridge Research Laboratories
Advanced Research Projects Agency

31 January 1973

AFCRL-TR-73-0057



# RESEARCH IN SEISMOLOGY

by
Carl Kisslinger and Otto W. Nuttli

Department of Earth and Atmospheric Sciences
Saint Louis University
St. Louis, Missouri 63103

Contract No. F19628-70-C-0036
Project No. 8652

## FINAL REPORT

Period Covered: 1 September 1969 through 31 December 1972
31 January 1973

Contract Monitor: Stanley M. Needleman
Terrestrial Sciences Laboratory



Approved for public release; distribution unlimited.

Sponsored by
Defense Advanced Research Projects Agency
ARPA Order No. 0292

Air Force Cambridge Research Laboratories
Air Force Systems Command
United States Air Force
Bedford, Massachusetts 01730

ARPA order no. 0292

Program code no. 0F10
Contractor:
Saint Louis University

Effective date of contract:
1 September 1969

Contract No. F19628-70-C-0036

Principal investigator and phone no.
Dr. Otto W. Nuttli/314-535-3000 - Ext. 547B

AFCRL project scientist and phone no.
Stanley M. Needleman - 617 861-3667

Contract expiration date 31 December 1972

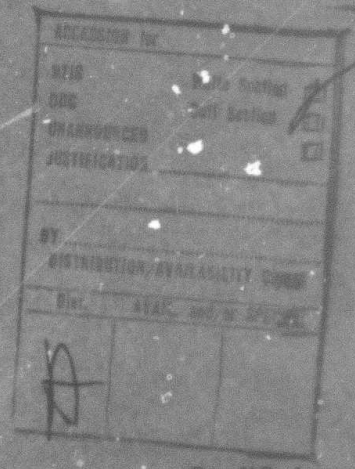

Unclassified

Security Classification

**DOCUMENT CONTROL DATA - R & D**

*(Security classification of title, body of abstract and indexing annotation must be entered when the overall report is classified)*

1. ORIGINATING ACTIVITY (Corporate author)
Saint Louis University
Department of Earth and Atmospheric Sciences
St. Louis, Missouri 63103

2a. REPORT SECURITY CLASSIFICATION

2b. GROUP

3. REPORT TITLE

RESEARCH IN SEISMOLOGY

4. DESCRIPTIVE NOTES (Type of report and inclusive dates)
Scientific Final 1 September 1969 - 31 December 1972 Approved 22 Feb. 1973

5. AUTHOR(S) (First name, middle initial, last name)
Carl Kisslinger
Otto W. Nuttli

6. REPORT DATE
31 January 1973

7a. TOTAL NO. OF PAGES
41

7b. NO. OF REFS
22

8a. CONTRACT OR GRANT NO.
F 19628-70-C-0036, ARPA Order No. 0292

b. PROJECT NO.
8652

c. DoD Element 62701D

d. DoD Subelement n/a

9a. ORIGINATOR'S REPORT NUMBER(S)

9b. OTHER REPORT NO(S) (Any other numbers that may be assigned this report)
AFCRL-TR-73-0057

10. DISTRIBUTION STATEMENT
A - Approved for public release; distribution unlimited.

11. SUPPLEMENTARY NOTES
This research was supported by Advanced Research Projects Agency.

12. SPONSORING MILITARY ACTIVITY
Air Force Cambridge Research Laboratories (LW)
L. G. Hanscom Field
Bedford, Massachusetts 01730

13. ABSTRACT

This report contains a summary and analysis of the results of research concerned with:

1. Seismic source properties, including spectral characteristics, focal mechanism and source dimension of earthquakes and explosions, and near-field ground motion and yield estimates.

2. Problems related to magnitude determination, particularly for small seismic events.

3. Problems related to the accurate location of seismic events.

DD FORM 1 NOV 68 1473



Unclassified

Security Classification

| 14. KEY WORDS | LINK A | | LINK B | | LINK C | |
|---|---|---|---|---|---|---|
| | ROLE | WT | ROLE | WT | ROLE | WT |
| Seismology | | | | | | |
| Earthquake magnitude | | | | | | |
| Explosion magnitude | | | | | | |
| Earthquake spectra | | | | | | |
| Earthquake mechanisms | | | | | | |
| Explosion mechanisms | | | | | | |
| Seismic wave amplitudes | | | | | | |
| Seismic velocities | | | | | | |
| Seismic travel times | | | | | | |

AFCRL-TR-73-0057

# RESEARCH IN SEISMOLOGY

by
Carl Kisslinger and Otto W. Nuttli

Department of Earth and Atmospheric Sciences
Saint Louis University
St. Louis, Missouri 63103

Contract No. F19628-70-C-0036
Project No. 8652

## FINAL REPORT

Period Covered: 1 September 1969 through 31 December 1972
31 January 1973

Contract Monitor: Stanley M. Needleman
Terrestrial Sciences Laboratory



Sponsored by
Defense Advanced Research Projects Agency
ARPA Order No. 0292

**Air Force Cambridge Research Laboratories**
**Air Force Systems Command**
**United States Air Force**
**Bedford, Massachusetts 01730**

ic

# SUMMARY OF RESEARCH RESULTS

## Introduction.

The research in seismology carried out under Contract F 19628-70-C-0036 can be divided into three broad categories for the purpose of summarizing and analyzing the results:

1. Seismic source properties, including spectral characteristics, focal mechanism and source dimension of earthquakes and explosions, and near-field ground motion and yield estimates.

2. Problems related to magnitude determination, particularly for small seismic events.

3. Problems related to the accurate location of seismic events.

Included under these broad categories are a large number of individual studies. Most have been completed and published or submitted for publication in seismological and geophysical journals, and three have been the basis of Ph.D. dissertations which were accepted by the Department of Earth and Atmospheric Sciences of Saint Louis University.

The presentation of this Final Report will be by way of a summary of the principal research results under the three headings mentioned above and an analysis of their significance. As further documentation of this summary and analysis, the abstracts of all published papers and dissertations are given in Appendices I and II, respectively. Appendix III contains synopses of other work carried out in the later months of the contract that has not reached the stage of readiness for publication but which has produced definite results which merit mention in this report.

## 1. Seismic Source Properties.

Under the general heading of Seismic Source Properties are included the spectral characteristics of certain small-magnitude earthquakes, focal mechanism and source dimension of selected earthquakes and explosions, and near-field motion and yield estimates for explosions.

### 1a. Spectral characteristics.

A study of the spectral content of 17 earthquakes in the New Madrid Seismic Zone (northeast Arkansas, southeast

Missouri and southwest Illinois) indicated that these earthquakes could be divided into two classes, one of which is deficient in low-frequency energy. This result was shown not to depend on the kind of seismograph system used to record the ground motion, or on the particular method used to obtain the spectrum. For example, the spectra were determined by both digital and analog methods. The earthquakes in question had body-wave magnitudes in the range $3\frac{1}{2}$ to $4\frac{1}{2}$. Although precise determinations of focal depth are lacking, all the earthquakes are known to have occurred in the upper half of the crust. (Rodriguez and Kisslinger, Appendix I-1). Theoretical studies based on dislocation theory indicate that certain models which include frictional forces on the fault surface yield P and S wave spectra that are peaked at intermediate frequencies (Rodriguez, Appendix III. 1).

A different approach was employed to study the source spectrum of deep-focus South American earthquakes. By using seismograms from stations near the epicenter, the transmission path of P waves from source to station is short. After the effects of propagation through a dipping crustal layer are removed by means of a method developed by Rogers and Kisslinger (Appendices I. 2 and II. 1), the resulting spectrum is that of the motion in the top of the mantle above the focus. To the extent that attenuation along the relatively short path from source to the top of the mantle can be ignored, the spectrum represents the source spectrum. Application of this methodology to the data of 7 earthquakes recorded at 4 stations indicates that in general the deduced spectrum of the P wave motion is flat at the low-frequency end and decreases as $f^{-2}$ at the high-frequency end. One exception to this statement was noted, namely the P-wave spectrum calculated from the Antofogasta seismograms for the earthquake of 5 March 1965, which was peaked at the intermediate frequencies (Somayajulu, Appendix III. 2).

An examination of the spectral content, in the frequency band from 0.05 to 1.0 Hz, of explosion-generated waves supports the generally-accepted conclusion that the ratio of high-frequency energy content to low-frequency energy content in explosive sources is large. The greatest uncertainty in the calculated source spectrum results from imperfect knowledge of the absorption of the high-frequency energy as it is transmitted through the earth's mantle. (Bennett, Appendix II. 2).

Spectra of long-period Rayleigh waves were used to determine the direction and dimensions of faulting for a selected group of earthquakes (Udias, Appendix I. 3).

Important conclusions. Insofar as VELA Uniform objectives are concerned, it is important to know that two classes of mid-continental, shallow-depth, small-magnitude earthquakes exist. The class which is relatively deficient in low-frequency energy will be indistinguishable from explosions, if only the $m_b - M_s$ discrimination criterion is employed.

1b. Focal mechanism and source dimensions of earthquakes and explosions.

From a study of the focal mechanism of earthquakes in the Delarof-Andreanof Island region of the Aleutian Islands, Stauder (Appendix I. 4) has demonstrated that the Aleutian Islands are active by independent blocks, and that the boundaries of these blocks are permanent features. One such boundary is Amchitka Pass, which separates the Rat and Andreanof Islands.

A study of a large number of small-magnitude aftershocks which followed the nuclear explosion BENHAM indicated that the fault-plane motion of these aftershocks can be related to the general fault trends of the Nevada Test Site area. Furthermore, the aftershocks of BENHAM follow the same recurrence rate as the aftershocks of earthquakes of the region. (Stauder, Appendix I. 5).

The focal mechanism solution of the Illinois earthquake of 9 November 1968 indicated reverse faulting on a N-S striking fault plane, which would correspond to E-W regional compressive stresses. (Stauder and Nuttli, Appendix I. 6). A similar stress pattern was found for New York earthquakes by Lamont-Doherty seismologists. Such a stress pattern is of the type that would be expected from the theory of plate tectonics for the interior of a continental plate.

A statistical decision-theory method, which utilizes as input data the sense of first motion of P waves, the amplitudes of P waves and the polarization of S waves, was developed to determine focal mechanism solutions. The method was applied to a set of Peruvian earthquakes, from which the stress pattern in the subduction zone was determined. (Wagner, Appendix II. 3).

Duda (Appendix I. 7) defined the boundary of the earthquake or explosion volume to be that surface on which the strain attains some critical value. Accepting Benioff's idea that the volume of space in which the aftershocks occur defines the volume of the principal or main shock, Duda shows that a strain of $10^{-6.5}$ would adequately represent the initial value. He further showed that the earthquake volume decreases with an increase of

focal depth, if the magnitude remains constant. Using published values of the distance separating the inelastic and elastic zones of nuclear explosions, Duda estimated that this boundary occurs where the strain is of the order of $10^{-4}$.

Important conclusions. From the point of view of concern about nuclear explosions triggering earthquakes, it is important to note that there are distinct seismic blocks in the Aleutian Islands which are seismically decoupled from each other. Presumably this is not peculiar to the Aleutian Islands, but occurs elsewhere. In addition to applying to subduction zones such as the Aleutians, the finding probably also holds for segments of oceanic ridges separated by transform faults.

Another important finding is that the theory of plate tectonics appears to explain the observed focal mechanism of earthquakes occurring in ridges, subduction zones and the interior of continents. This makes it possible to readily correct earthquake magnitudes for focal mechanism, as will be explained in section 2. Furthermore, extending by analogy the results found for eastern North America, the earthquakes which occur in the interior of the Eurasian plate should be of the reverse thrust type, with fault plane and auxiliary plane dipping at about $45^{\circ}$. This will result in compressions for the direction of the P motion at teleseismic distances in all azimuths, which will tend to cause these earthquakes to be confused with explosions.

From Duda's (Appendix I.7) relation between magnitude, strain and epicentral distance, it should be possible to predict the strain levels at any desired distance for an explosion of a given yield.

1c. Yield and near-field ground motion estimates for underground explosions.

A relatively simple relation appears to hold between the yield of underground nuclear explosions and the maximum value of the amplitude/period ratio of the vertical component of Rayleigh waves in the period range of 5 to 12 seconds. Eighteen NTS explosions were studied, seven of known yield and eleven of unknown yield. For the seven events of known yield, the average of the yield as determined from the Rayleigh-wave motion at eight stations agreed within one standard deviation of the known yield. (Wagner, Appendix I. 8).

Attenuation formulas for surface waves generated by a point source, together with observations of body-wave and surface-wave magnitudes by conventional methods from data obtained at teleseismic distances, can be used to

predict the maximum ground motion and particle velocity on hard rock resulting from underground explosions, at distances of 100 to 500 km. The procedure for making such calculations, heretofore unpublished, is briefly described in Appendix III. 3 (Nuttli). The underlying theory is given in a paper by Nuttli (Appendix I. 9). The method was applied to CANNIKIN, with the following results: $\Delta$ = 305 km, $v_z$ (max) = 2.2 mm/sec (calculated) and 2.2 mm/sec (observed); $\Delta$ = 370 km, $v_z$(max) = 1.9 mm/sec (calculated) and 2.3 mm/sec (observed); $\Delta$ = 305 km, $A_z$ (max) = 0.58 mm (calculated) and 0.63 mm (observed); $\Delta$ = 370 km, $A_z$ (max) = 0.85 mm (calculated) and 0.60 mm (observed).

Important conclusions. The procedures described above permit one to estimate the yield of underground NTS explosions from the $(A/T)_{max}$ values of the vertical component of Rayleigh waves recorded at distances of thousands of kilometers, and apparently do not depend greatly on the source medium. They also permit one to estimate maximum displacements and particle velocities in hard rock at distances of 100 to 500 km if the body and surfave wave magnitudes are known from measurements at teleseismic distances, or, equivalently, if the yield is known.

## 2. Magnitude Determination.

Magnitude determination problems include those related to the attenuation of wave energy, the excitation of waves of a given frequency (source spectrum) and the non-uniform azimuthal radiation of wave energy.

### 2a. Attenuation of P waves.

There are two ways of approaching the problem of the amplitude vs distance relation for P waves. One is to assume a knowledge of the velocity vs depth and the Q values in the mantle, and calculate the amplitude vs distance curve (Duda, Appendix I.10 and Bennett, Appendix II.2). Duda used the velocity vs depth relation based on the Herrin 1970 P Tables, and assumed no anelastic attenuation. Bennett included absorption in his earth model, but found that the assumption that Q is independent of frequency led to results which contradict observations at frequencies of about 1 Hz.

A different approach was taken by Nuttli (Appendix I.11), who made use of observational data of P wave amplitudes, measured in the time domain, for large explosions in Nevada, Amchitka and Novaya Zemlya, as recorded by long- and short-period, vertical-component WWSSN seismographs. For the long-period seismograph data the amplitude vs

and have developed tables for earthquakes in Kamchatka, the Aleutians and the Mid-Atlantic which indicate the stations whose data are to be used for obtaining the magnitude. Tables give the error in $m_b$ to be expected if the amplitude data of a single point, such as LASA, are used for the estimate of magnitude, for earthquakes in the regions listed above.

Appendix I.13 (Syed, Kisslinger and Nuttli) presents a discrimination technique based on the above ideas. An explosion will appear anomalous, because its radiation pattern differs from that of a typical earthquake in the region where it occurs. The test is straightforward, in that it requires only P-wave amplitude data from a number of stations well distributed in azimuth. Before it can be applied to events in a given region, the prevailing focal mechanism for earthquakes in that region must be known. This information can be obtained from seismic studies of focal mechanism or predicted by the theory of plate tectonics.

Important Conclusions. The method provides a simple discriminant between earthquakes and explosions, which does not require sophisticated calculations and which therefore can be applied to test a large number of events. The only seismological data required are the P-wave amplitudes at a number of azimuths.

Relatively large errors in $m_b$ determination can result from using the amplitude data of only a few stations or arrays to calculate magnitude. The method described above enables one to correct such data for the focal mechanism of earthquakes.

3. Location of Seismic Events.

Accurate location of seismic events requires a knowledge of the travel times of seismic waves and their lateral variations. The research described below is concerned with travel times and velocity structure in eastern North America, and with lateral variation in the low-velocity channel for shear waves in the western United States.

3a. Travel times and velocities in eastern North America.

Earthquakes and chemical explosions in the central United States provided data on the velocity structure of the crust and upper mantle in eastern North America. These data were summarized by Nuttli, Stauder and Kisslinger (Appendix I.14), who used them to calculate travel-time tables for the region. These tables now are used routinely by Saint Louis University and the National Oceanic and Atmospheric Administration for the location of mid-continent earthquakes.

distance curve closely resembled that of Duda (Appendix I.10), which implies very small values of absorption for P waves whose rays bottom below the low-velocity channel in the upper mantle. For the short-period seismograph data the amplitude vs distance relation showed some influence of absorption, out to distances of about 5000 km. The magnitude calibration curve obtained from the data of this study differs from the standard Gutenberg-Richter calibration curve principally at distances of about 4000 to 5000 and 6500 to 7500 km.

Important Conclusions. In order for the $m_b$ vs $M_s$ relation to be a reliable discriminant between earthquakes and explosions, it is necessary that the $m_b$ and $M_s$ values of the event be accurately known. The present studies indicate that the Gutenberg-Richter calibration curve gives an average magnitude which will not differ by more than 0.1 $m_b$ unit, if data are available over a large range of epicentral distances, such as is the case for large-magnitude earthquakes and explosions. However, for small-magnitude events, which may be detected by only a few arrays or special high-magnification stations, underestimates of $m_b$ by as much as 0.4 units can occur from the use of the Gutenberg-Richter curve at distances of 4000 to 5000 km.

2b. Attenuation of surface waves.

Nuttli (Appendix I.9) studied the attenuation of short-period (1 sec) and intermediate-period (3 to 12 sec) surface waves, and presented formulas for calculating $m_b$ from the short-period waves and $M_s$ from the intermediate-period waves. These formulas yield magnitudes which are consistent with $m_b$ and $M_s$ values obtained in the conventional manner, from the amplitudes of P waves and 20-second period surface waves recorded at teleseismic distances. Nuttli's amplitude data, as well as those which form the bases of Richter's $M_L$ magnitude scale and Gutenberg-Richter's $M_S$ magnitude scale, are shown to be consistent with the theory of a point source of dispersed surface waves traveling over the surface of a sphere. However, $M_s$ formulas proposed by Evernden and by Basham, utilizing the amplitudes of approximately 10 to 15 sec period $R_g$ waves, are shown to be inconsistent with the theory in that they require zero, or even negative, absorption. One possible explanation of their data is that the phase whose amplitude they are measuring results from the constructive interference of fundamental and higher-mode waves of the same period and group velocity. If this is the correct explanation, then their formulas will only be valid for those regions where the crust-mantle structure gives rise to the same group velocity relation. The phase which they measured is not seen, for example, for eastern North American earthquakes recorded by stations in eastern North America.

Important Conclusions. Formulas have been developed which enable one to compute $m_b$ and $M_s$ for small-magnitude events in eastern North America, for $m_b$ values down to about 3 and $M_s$ values down to about 2.5. Considering the geological similarities between North America east of the Rocky Mountains and the interior of Eurasia, it is not unlikely that these formulas will apply also for the interior of Eurasia. However, this can only be established by studying the attenuation of surface waves generated by events within Eurasia and recorded by seismographs located in or at the edge of the stable interior of the continent.

2c. Relative excitation of short- and long-period waves.

The $m_b$ vs $M_s$ discrimination criterion assumes that all earthquakes of a given $m_b$ value will have a constant $M_s$ value, i.e., that their source spectra are the same. In section 1a. of this report (and in Appendix I.1) it was noted that this assumption is not satisfied for a certain class of New Madrid zone earthquakes, namely the group whose spectra are deficient in low-frequency energy. To determine the effect of such source spectrum differences on the $m_b$ vs $M_s$ relation, a study of the relation between the magnitudes was made for recent earthquakes in the Central United States (Nuttli, Appendix III.4). From the study it was found that the $M_s$ value of the 1 October 1971 earthquake, an earthquake which Rodriguez and Kisslinger (Appendix I.1) found to be deficient in low-frequency energy, was 0.4 units less than that to be expected from the $m_b$ vs $M_s$ relation for the "ordinary" earthquakes of the region. The expected value is $M_s = 3.05$, and the observed value $M_s = 2.65$.

Important Conclusions. Earthquakes whose source spectra are deficient in low-frequency energy have correspondingly low $M_s$ values. They likely would be confused with explosions, on the basis of the $m_b$ vs $M_s$ criterion.

2d. Dependence of wave amplitudes on focal mechanism.

The focal mechanism of earthquakes results in a dependence of wave amplitude on azimuth and distance, which is in addition to the amplitude vs distance fall-off used in calculating magnitudes. This phenomenon is not very important when the data of a large number of stations are used to determine an average magnitude, resulting in general in only a larger value of the standard deviation.

Syed and Nuttli (Appendix I.12) and Syed (Appendix II.4) have shown that there is a consistency of focal mechanisms for earthquakes in a given geographic region,

and have developed tables for earthquakes in Kamchatka, the Aleutians and the Mid-Atlantic which indicate the stations whose data are to be used for obtaining the magnitude. Tables give the error in $m_b$ to be expected if the amplitude data of a single point, such as LASA, are used for the estimate of magnitude, for earthquakes in the regions listed above.

Appendix I.13 (Syed, Kisslinger and Nuttli) presents a discrimination technique based on the above ideas. An explosion will appear anomalous, because its radiation pattern differs from that of a typical earthquake in the region where it occurs. The test is straightforward, in that it requires only P-wave amplitude data from a number of stations well distributed in azimuth. Before it can be applied to events in a given region, the prevailing focal mechanism for earthquakes in that region must be known. This information can be obtained from seismic studies of focal mechanism or predicted by the theory of plate tectonics.

Important Conclusions. The method provides a simple discriminant between earthquakes and explosions, which does not require sophisticated calculations and which therefore can be applied to test a large number of events. The only seismological data required are the P-wave amplitudes at a number of azimuths.

Relatively large errors in $m_b$ determination can result from using the amplitude data of only a few stations or arrays to calculate magnitude. The method described above enables one to correct such data for the focal mechanism of earthquakes.

3. Location of Seismic Events.

Accurate location of seismic events requires a knowledge of the travel times of seismic waves and their lateral variations. The research described below is concerned with travel times and velocity structure in eastern North America, and with lateral variation in the low-velocity channel for shear waves in the western United States.

3a. Travel times and velocities in eastern North America.

Earthquakes and chemical explosions in the central United States provided data on the velocity structure of the crust and upper mantle in eastern North America. These data were summarized by Nuttli, Stauder and Kisslinger (Appendix I.14), who used them to calculate travel-time tables for the region. These tables now are used routinely by Saint Louis University and the National Oceanic and Atmospheric Administration for the location of mid-continent earthquakes.

A study of the travel times of P waves from the 9 November 1968 Illinois earthquake (Stauder and Nuttli, Appendix I. 6) showed significant regional differences in travel times to distances as great as about 2500 km, corresponding to rays which bottom in the upper 700 km of the earth's mantle. Beyond this distance regional differences in station location have little effect upon the total travel time.

Aftershock studies of the 9 November 1968 earthquake (Stauder and Pitt, Appendix I. 15) showed that the earthquake had anomalously low aftershock activity, which is true of most earthquakes in northern Illinois and southeast Missouri.

3b. S-wave low-velocity channel.

Shear wave travel-time residuals, equalized with respect to the residuals at Albuquerque, have been determined for the WWSSN and LRSM stations in the western United States, for a set of Japanese and a set of South American earthquakes (Yasar, Appendix III. 6). The resulting residuals have been interpreted in terms of changes of thickness of the low-velocity channel for shear waves. When completed, the study will provide information on the velocity structure in the channel and a contour map of the depth to the top of the channel.

Important Conclusions. The research discussed in section 3 is of the type needed to improve epicentral location, and to correct travel times and amplitudes for the effects of crustal and upper mantle structure.

## Appendix I. Abstracts of Publications Resulting from Research Done under This Contract.

I.1 Rodriguez, Rene and Carl Kisslinger, 1972, Spectral classification of New Madrid earthquakes: EOS, Transactions American Geophysical Union, 53, 450. (Abstract of paper presented at 1972 meeting of American Geophysical Union.)

Analyses of the spectra of earthquakes in the New Madrid seismic zone have revealed that a group of these is characterized by the absence of long-period energy and by relatively high corner frequencies. Seventeen earthquakes in the magnitude range $m_b$ 1.7 to 4 have been examined, using the data of the western Tennessee seismic network. The larger events have also been analyzed at near-regional distances from the seismograms of permanent observatories. Pairs of earthquakes with about equal $m_b$ values have significantly different $M_s$ values, small for the high frequency events. The area of perceptibility depends on the spectral class of the earthquake, with the high frequency events felt and recorded only over small distances compared to the normal events.

I.2 Rogers, Jr., Albert M., and Carl Kisslinger, 1972, The effect of a dipping layer on P-wave transmission: Bulletin of the Seismological Society of America, 62, 301-324.

A ray-theory development of the effect of dip on P-wave transmission through a single layer over a half-space permits an assessment of errors due to dip in estimates of crustal thickness from observed P-wave spectral properties using transmission coefficients for a nondipping interface. The possibility of simultaneously deriving depth and dip from such observations is also shown. The theory has been tested by experiments in a two-dimensional laboratory model and applied to observations of deep South American earthquakes at small epicentral distances.

Theory and laboratory results show that errors in depth reflecting dip are less than 5 per cent for dips up to 25°. Dip can be estimated by matching observed and theoretical curves, once a velocity contrast has been fixed independently. A curve-matching technique for objectively selecting the best match has been developed.

A variation of parameter study shows that changes in velocity contrast do not change the shape of the crustal transfer function, but peak-to-trough

differences increase with increasing velocity contrast. A change in depth of a dipping layer produces no change in the crustal transfer function plotted in dimensionless frequency. The transfer function changes with dip more rapidly for waves incident downdip. If the data window is long enough to include P and PPP (three P legs in the layer), the depth determination is not sensitive to window length, but dip determination is not possible for short windows.

The data for Antofagasta permit one of two solutions, a crust either 46.1 or 56.7 km thick, with the M discontinuity dipping $5^{\circ}$ east, with the 46.1 km thickness preferred. This result agrees well with refraction results of others. A less firm result for Nana is a crust 74.7 km thick, with dip $15^{\circ}$ to the southeast.

I.3 Udias, Agustin, 1971, Source parameters of earthquakes from spectra of Rayleigh waves: Geophysical Journal of Royal Astronomical Society, 22, 353-376.

A generalized form of the directivity function has been used to determine the length and the rupture velocity of four earthquakes with known vertical strike slip faulting. For body wave magnitudes between 5.7 and 7.0, the lengths vary from 18 to 35 km with a rupture velocity of 1.5 $kms^{-1}$. Seismic moments have been determined from the spectral amplitude densities and the theoretical response to a point source model. From these values, stress drops of 2 to 30 bars and average dislocations of 4 to 160 cm have been derived. The products of the average stresses acting at the fault by the seismic efficiency factor are of the order of $10^{7}$ dyne $cm^{-2}$ for all four earthquakes; this seems to indicate a minimum strength of the crust under horizontal shear stress of the same order.

I.4 Stauder, William, 1972, Fault motion and spatially bounded character of earthquakes in Amchitka Pass and the Delarof Islands: Journal of Geophysical Research, 77, 2072-2080.

During the period from May 1969 to March 1970, seven moderate earthquakes occurred in the Delarof-Andreanof Island region. The focal mechanisms of these earthquakes correspond to the motion that would be expected on the basis of plate tectonics. Of more particular significance, the motion in one of these shocks, located at intermediate depth in the Benioff

zone, indicates horizontal tension parallel to the plate, corresponding to lateral extension as the plate descends under an arcuate structure convex to the plate motion. The spatial and temporal relation of these earthquakes and of their aftershock sequences to the over-all activity of the arc and particularly to the seismicity of the Rat Islands during this period supports the hypothesis that the Aleutian Islands are active by independent blocks and that the boundaries of these blocks are permanent features.

I.5 Stauder, William, 1971, Smaller aftershocks of the Benham nuclear explosion: Bulletin of the Seismological Society of America, 61, 417-428.

The examination of the BENHAM aftershocks is extended to 162 earthquakes approximately an order of magnitude smaller than those previously studied. The spatial distribution of these smaller events is similar to that found for larger events examined by Hamilton and Healy (1969). Focal mechanisms are also similar to those of the larger aftershocks: dip-slip along northeasterly trending zones and generally strike-slip along a north-south trending zone west of the shot-point. About one third of the mechanism solutions are ambiguous, capable of either interpretation. Amplitude data are successfully used to resolve the ambiguity in about one half of these cases by selecting the solution which gives a notably lesser value of the variance, $\sum (A_{i,obs} - kA_{i,calc})^2/N$ of the amplitude residuals. The value of $k$ is related to the magnitude of the shocks. A b value of 1.09 indicates that aftershocks of the explosion follow a recurrence rate normal for regional earthquakes or aftershock sequences.

I.6 Stauder, William and Otto W. Nuttli, 1970, Seismic studies: south central Illinois earthquake of November 9, 1968: Bulletin of the Seismological Society of America, 60, 973-981.

The largest earthquake to occur in the central Mississippi seismic region this century took place in south central Illinois on November 9, 1968. The hypocenter and origin time based on observations from twelve regional stations varying in epicentral distance from 171 to 549 km, are $37.95^{o}$N, $88.48^{o}$W, h = 25 km, O = $17^{h}01^{m}42.0^{s} \pm 0.2^{s}$.

Travel times of P at stations distant less than 2600 km indicate regional mantle variations, corresponding to rays bottoming at depths down to 650 km. Beyond this point travel times show a much smaller dependence, if any, on region. For stations in the

central United States P times may be fitted by two straight line branches which intersect at about 600 km. The first branch corresponds to $P_n$, the second to rays refracted from a surface at depth 97 km with a velocity below it of 8.35 km/sec. At larger distances ($48^o$-$100^o$) there are non-azimuth dependent residuals with respect to the Herrin Tables averaging about -1.5 sec, indicating a source-region correction with respect to these tables.

Body wave magnitude was determined to be $m_b$ = 5.54 ± 0.44 for stations for which $\Delta > 25^o$, and $m_b = \overline{5}.44 \pm 0.29$, using Evernden's formula, for $P_n$ in eastern North America. Surface waves give a value $M_S$ = 5.2.

The fault plane solution determines two nodal planes each striking approximately north-south and dipping $45^o$ to the east and to the west, respectively. This corresponds to dip slip, reverse motion, and to a horizontal east-west axis of compressional stress. While there are no mapped faults in the immediate epicentral region, the motion indicated is in conformity to that along the Wabash Valley Fault System 10 miles to the east.

I.7 Duda, Seweryn J., 1972, Body-wave strain and the earthquake volume: Tectonophysics, 14(3/4): 333-343.

The strain produced by body waves in the vicinity of the earthquake is employed in the definition of the earthquake volume. The definition is applicable to artificial seismic events. Distances from the focus at which a given maximum strain was attained during the event, are presented as a function of magnitude and focal depth. The computed strains are compared with strains measured and reported for a number of earthquakes and nuclear explosions. The earthquake volume shows a distinct decrease with focal depth. The strains produced by body waves during the earthquake throw some light on the stress state in the vicinity of the focus, and are considered to be able to yield information of the rate of tectonic strain accumulation.

I.8 Wagner, Donald E., 1970, Nuclear yields from Rayleigh waves: Earthquake Notes, XLI, No. 3, 9-20.

Maximum A/T ratios of Rayleigh waves are measured at continental WWSSN stations to predict nuclear yields of eleven events at the Nevada Test Site. A revision of Richter's surface wave magnitude to $M_S' = 2.4 + \log(A/T_{4-12}) + 1.66 \log(\Delta)$ is verified.

1.9 Nuttli, Otto W., 1973, Seismic wave attenuation and magnitude relations for eastern North America: Journal of Geophysical Research, 78,

Observational data on the attenuation of short-period Rayleigh waves in North America east of the Rocky Mountains yield the following average values for the coefficient of anelastic attenuation: $\gamma = 0.07$ deg$^{-1}$ for 1 sec period waves and $\gamma = 0.10$ deg$^{-1}$ for waves of maximum particle velocity in the 3 to 12 sec period range. By way of comparison, the amplitude data which form the basis of Richter's empirical local magnitude scale for southern California give $\gamma = 0.60$ deg$^{-1}$. Differences in $\gamma$ values are sufficient to explain the observed fact that earthquakes in the eastern United States have as much as a tenfold larger radius of perceptibility as earthquakes of the same magnitude in the western United States.

Theoretical curves of log A/T versus log $\Delta$ are not linear. Thus, magnitude formulas of the type $M = B + C \log \Delta + \log A/T$ are valid only over a limited range of distance, for which the curve can be approximated by a straight line. Formulas of this kind, which give $m_b$ and $M_s$ from short-period Rayleigh waves, are proposed for eastern North America.

1.10 Duda, Seweryn J., 1971/IV, Travel times and body wave magnitude: Pure and Applied Geophysics 87, 13-37.

Presently used $\overline{Q}$-charts for magnitude determinations have been obtained principally on the base of direct observations of ground motion amplitudes, and periods, of several components of seismic waves (such as PZ, PH, SH), as function of epicentral distance. However, observations alone can serve for the definition of a magnitude scale for events with only one particular focal depth. In order to make the magnitude concept applicable to all focal depths, it must be decided when two events with different focal depths should be assigned the same magnitude. Any respective decision which will assure consistent magnitudes, must be based on the velocity vs. depth, and eventually the anelasticity vs. depth profiles of the Earth.

It is concluded that in magnitude studies the anelasticity is of minor importance. Thus, after the amplitudes are compensated for the radiation pattern at the focus, the observed variation of amplitudes along the surface of the Earth, as function of epicentral distance, is practically due only to the velocity heterogeneity inside the Earth. Assuming a dependence of the velocity on the distance from the center of the Earth (no lateral velocity heterogeneities are permitted), a set of new Q-charts is obtained, independent of direct amplitude observations, for PZ-, PH-, and SH-waves. A refinement in the magnitude

definition warrants the magnitude figures obtained with the new $\overline{Q}$-charts to be uniform with regard to focal depths. Examples show the new $\overline{Q}$-charts to decrease the scatter of magnitude determinations between stations.

Since the efficiency in generating longitudinal and transverse waves is most probably not the same for all events, separate P-wave and S-wave magnitudes are advocated.

I.11 Nuttli, Otto W., 1972, The amplitudes of teleseismic P waves: Bulletin of the Seismological Society of America, 62, 343-356.

Amplitudes of P waves recorded by long-period seismographs for nuclear explosions in Novaya Zemlya, the Nevada Test Site, and Amchitka Island yield a new body-wave magnitude calibration function for teleseismic distances. At some distances, it differs from the Gutenberg-Richter (1956) function by as much as 0.4 magnitude units.

A comparison of short- and long-period body-wave magnitudes for the 1966 Novaya Zemlya event indicates that anelastic attenuation of P waves is greater in the upper than in the lower mantle, but, for waves with periods of 1 sec or greater, the effect of anelastic attenuation on the amplitudes is less than that of geometric spreading.

The amplitude data hint at the existence of a second-order velocity discontinuity in the lower mantle at a depth of about 2300 km.

I.12 Syed, Atiq A., and Otto W. Nuttli, 1971, A method of correcting P-wave magnitudes for the effect of earthquake focal mechanism: Bulletin of the Seismological Society of America, 61, 1811-1826.

This paper presents a methodology for correcting body-wave magnitudes for the effect of focal mechanism in a routine manner. The method requires a knowledge of the prevailing or dominant mechanism for a geographic region, from which tables are constructed which enable one to make the necessary correction. Included in the paper are tables for Aleutian Island, Kamchatka and mid-Atlantic Ocean earthquakes.

From a study of seven earthquakes, it is concluded that the present method gives essentially the same average magnitude with the same standard deviation as a more exact method of correcting for the focal mechanism. The latter method uses the focal-mechanism parameters of the earthquake, which must be determined independently for each earthquake.

The existing distribution of seismograph stations is such that transform-fault earthquakes of the mid-Atlantic Ocean will consistently have their P-wave magnitudes underestimated by about 0.2 magnitude units, if no correction is made for the focal mechanism. On the other hand, P-wave magnitudes of earthquakes in Kamchatka and south of the axis of the Aleutian Trench will be overestimated by about 0.2 units.

I.13 Syed, Atiq A., Carl Kisslinger and Otto W. Nuttli, 1971, A Seismic discriminant based on focal mechanism: Bulletin of the Seismological Society of America, 61, 1827-1830.

Utilizing the observation that a predominent focal mechanism exists for a given hypocentral region, a seismic discriminant based on body-wave magnitude has been developed. This discriminant enables one to identify earthquakes that do not fit mechanisms expected from plate tectonics. It also sorts out explosions as anomalies, even for those regions in which the focal mechanism results in compressional first motions at most or all available seismograph stations.

I.14 Nuttli, Otto W., William Stauder and Carl Kisslinger, 1969, Travel-time tables for earthquakes in the central United States: Earthquake Notes, 40, No. 4, 19-28.

Travel-time tables for earthquakes occurring in the central United States and recorded in central and eastern North America are presented for distances from 0 to 1000 km. The tables are given for focal depths of 0, 5, 15, 25 and 35 km.

I.15 Stauder, William, and Andrew M. Pitt, 1970, Note on an aftershock study, south central Illinois earthquake of November 9, 1968: Bulletin of the Seismological Society of America, 60, 983-986.

In an effort to monitor aftershock activity following the southern Illinois earthquake of November 9, 1968, a network of ten high gain seismic stations was established in the vicinity of the epicenter of the earthquake. The network began recording on the fourth day after the earthquake and operated for a period of ten days. During this time only one very small aftershock was recorded. The hypocenter of this shock was about 10 km south and at the same depth as that of the main shock.

Permanent stations of the region recorded two other aftershocks within two days of the main shock, and one more three and a half months later. The exceptionally low level of aftershock activity is an anomalous feature of the Southern Illinois-Southeast Missouri seismic zone.

## Appendix II. Abstracts of Ph. D. Dissertations Resulting from Research Done under This Contract

II.1 Rogers, Jr., Albert M., The effect of a dipping layer on P wave transmission, 1970.

A ray theory for the multiple reflection solution of plane waves propagating in a wedge overlying a half space is developed and evaluated as the parameters velocity contrast, crustal thickness, angle of emergence, angle of dip, and spectral resolution are varied individually.

An objective method for determining the "best fit" is developed using the correlation co-efficient. This technique is employed to determine the theoretical error in the depth determination that might be expected if one applies the Haskell-Thomson one layer model to an earth with a dipping one layer crust. The errors are evaluated for two representative angles of emergence as the dip varies and are found to be less than $\pm 7\%$ in all cases. However, there are a number of cases of "no fit."

A series of model experiments are conducted as a test of the ray theory, and to measure the accuracy attainable in the crustal thickness determinations by fitting transfer functions. It is demonstrated that the theory adequately describes the physical processes in the model within the approximations of the experiments themselves. The accuracy of the thickness determination for the experiments is about $\pm 1\%$.

The ray theory is also applied to crustal transfer functions obtained from South American stations. The crustal thickness at Antofagasta, Chile is found to be 46.1 km dipping $5^{\circ}$E, and at Nana, Peru a fit is found for a crust 74.7 km thick dipping $15^{\circ}$E.

II.2 Bennett, Theron J., Determination of source characteristics of underground nuclear explosions from analysis of teleseismic body waves, 1971.

One of the classical problems of seismology is the recovery of information about the source of seismic waves using observations made at large distances from the focus. In this dissertation we have used long-period seismograph records of the body waves from a relatively simple type of source, an explosion, and applied equalization techniques in an attempt to retrieve information about the energy release, the source dimensions, and the strain levels near the focus.

We performed a spectral analysis of seventy-five P-wave records and five S-wave records from eight large, underground nuclear explosions. The displacement

amplitude spectra in the frequency band from 0.05 to 1.0 Hertz were reduced to the source by application of the method of amplitude equalization. Estimates of the energy spectrum, cumulative energy spectrum, and strain spectrum on the focal sphere were derived for each event from the average displacement amplitude spectrum reduced to the focal sphere.

The total P-wave energy in the frequency band from 0.1 Hertz to 0.7 Hertz was computed for each explosion for four different absorption models and the results compared. The energy calculations were found to be strongly dependent on the choice of the absorption model. At the present time, the effect of absorption on body-wave amplitudes is not well understood and is the subject of much discussion. The results we present here emphasize the need for an accurate knowledge of the absorption behavior in amplitude studies.

The portion of the total P-wave energy to be expected in the limited frequency band from 0.1 to 0.7 Hertz was calculated on the basis of Sharpe's theory and was determined to be of the order of one-sixth for a typical model of a one megaton explosion. Seismic coupling factors were obtained by comparing observed energies to the yields measured independently. These results were again found to be critically dependent on the absorption model. The model which gave efficiencies of the order of $10^{-3}$ is recommended as being the most appropriate for describing the absorption in the frequency band from 0.1 to 0.7 Hertz; this model corresponds to the assumption that $(T/Q_{AV})$ equals one and a half seconds where T is the travel time of the ray. Relations between magnitude and band-limited energy and magnitude and yield were developed.

The strain level on the elastic-nonelastic boundary of an explosion was computed from the P-wave magnitude using a ray-tracing technique. The value of this strain was found to be approximately $10^{-4}$. Based on this same approach, the distance from the focus at which each explosion reached the same level was calculated. The results were compared to observations by others of the radius of the boundary between elastic and nonelastic behavior based on Sharpe's theory and to the relative size of the nonelastic zone obtained by comparing the levels of the strain spectra on the focal sphere. The correlation seems to be fairly good.

II.3 Wagner, Donald E., Statistical decision theory applied to the focal mechanisms of Peruvian earthqiakes, 1972.

A statistical decision theory was developed to determine earthquake focal mechanisms for nine shallow, four intermediate, and five deep focus events which occurred in northwestern South America. The theory combines the independent body wave measurements of P-wave first motions, S-wave polarization angles, and dominant P-wave amplitudes from long-period WWSSN stations.

Nodal plane solutions were calculated in the following manner: Observed P-wave polarities were plotted on a stereographic projection and a trial solution was chosen which minimized the number of quadrant inconsistencies for a theoretical double-couple source. Next, this graphical solution was perturbed in azimuth and/or dip until a solution set of all possible pairs of orthogonal nodal planes which differed by at least one degree and which allowed no further inconsistencies was generated. Finally, the observations of P amplitudes and S polarization angles were combined to statistically choose a solution from the set of orthogonal nodal planes.

To combine the P amplitudes and S polarization angles, a linear cost function formalism was developed. At each station, the residual between the measured and theoretical S polarization angle and the measured and theoretical P amplitude was computed for all the pairs of nodal planes in the solution set. This residual or quantitative error was then converted to a dollar-and-cents value through a cost coefficient. That is, a residual of X degrees in the polarization angle was assigned a value of Y dollars. Large residuals were assigned higher values than smaller ones. Because the P and S residuals were both converted to a common metric (i.e., value), it was possible to combine them via a single linear cost function. Therefore, the optimum nodal plane solution was chosen as that solution which minimized the linear cost function.

The above procedure was applied to determine the focal mechanisms of eighteen Peruvian earthquakes. These mechanisms were categorized according to focal depth. The five deep inland events on the Peru-Brazil, Peru-Bolivia border demonstrate near-vertical principal pressure axes. In central Peru and Ecuador four intermediate depth events indicate a clustering of principal tension axes dipping at $45^{o}$. Moreover, these tension axes plunge in a NE to SE direction perpendicular to the Peruvian Trench. Nine shallow focus events display a wide range of solutions. In the

Peruvian Trench, four earthquakes are found to have horizontal principal axes which strike perpendicular to the trench axis, while one earthquake yields a thrust fault mechanism. Two events in Ecuador and Colombia reveal a strike-slip mechanism with a possible slip axis perpendicular to the trench. Finally, two events in north central Peru show horizontal principal pressure axes.

These solutions are accounted for by the following model: An oceanic lithosphere approximately 70 km thick is dipping under the South American continent at the Peruvian Trench. To the east of the trench is a continental lithosphere. The oceanic lithosphere acts as a stress guide which changes the direction of principal stresses within the slab such that they align parallel to the dip of the descending lithospheric plate. Earthquakes occur in response to the state of stress within the slab which is in turn characterized by the principal stresses. Therefore, the four intermediate depth events with tension axes parallel to the plate indicate the lithosphere is in extension. This is interpreted as the gravitational sinking of an unstable oceanic lithosphere into the underlying asthenosphere. On the other hand, the five deep events with vertical pressure axes demonstrate that the lithosphere is in compression below 550 kilometers. We interpret this as a segment of lithosphere which has possibly separated from the intermediate depth lithosphere and whose downward motion is now being retarded by the surrounding mantle. Finally, the nine shallow focus events illustrate a wide range of tectonic activity. Their focal mechanism solutions indicate possible thrusting of the oceanic lithosphere under the continental lithosphere, transform faults perpendicular to the Peruvian Trench axis, and mechanical instabilities related to the bending of an oceanic lithospheric plate.

II.4 Syed, Atiq A., Effects of the earthquake source mechanism on P wave magnitude determination, 1971.

The mechanism at the focus of an earthquake is an important factor in determining the energy radiated in different directions and its distribution into different wave types. The purposes of this study are to provide a quantitative estimate of the effect of the earthquake radiation pattern on the recorded body wave amplitudes, and to develop a routine procedure for obtaining body wave magnitude estimates corrected for focal mechanism. A closely related problem of developing criteria for sorting out those earthquakes whose focal mechanisms are not adequately represented by the assumed dominant one also is considered.

In order to accomplish these objectives, the published focal mechanism solutions of 88 earthquakes in the Aleutian Islands, Kurile Islands-Kamchatka region and the mid-Atlantic Ocean have been compiled. These seismically active areas have been divided into eight subregions, on the basis of the similarity of the focal mechanism of earthquakes in each of these subregions. The prevailing or dominant focal mechanism parameters have been calculated, by taking the average of the focal mechanism parameters of the earthquakes forming each subregion.

On the basis of the dominant focal mechanism, selection of seismograph stations which will record relatively large P wave amplitudes (larger than the average amplitude at the focal sphere) from earthquakes in each subregion has been carried out. Regional corrections, to account for the radiation pattern of the predominant focal mechanism in the hypocentral region, have been established. Our calculations indicate that the number of stations expected to record relatively large P wave amplitudes is maximum when the dominant focal mechanism corresponds to the B axis being almost horizontal, and minimum when the B axis is almost vertical. In these cases, by disregarding the effect of focal mechanism, body wave magnitudes will be overestimated or underestimated by about 0.2-0.3 magnitude units, respectively.

The validity of the proposed method has been tested using the first arriving, long period P wave amplitude data of ten earthquakes in various subregions. A comparison of the average $m_b$ value obtained by using the P wave amplitude data of all the stations, with the corresponding $m_b$ value obtained using data at only the selected stations, indicates that the second set of $m_b$ value shows less scatter than the first set in all cases studied.

A method of sorting out the earthquakes or events whose focal mechanism does not correspond to the dominant mechanism has been developed. This method has been tested using the P wave amplitude and period data of seven earthquakes. It was possible to establish the validity of the calculated dominant mechanism in six cases. In the seventh case the prevailing mechanism was found to differ from the actual mechanism, which was determined independently.

## Appendix III. Synopses of Research Done under This Contract but Not Yet Published.

### III.1 Friction and the mechanism of shallow focus earthquakes, by Rene Rodriguez.

Recent theoretical and experimental studies of earthquake source models indicate that the inclusion of friction in the models leads to a better understanding of some of the physics of faulting, especially for shallow earthquakes. Such an understanding should provide useful information for predicting and perhaps ultimately controling earthquakes.

Friction is included in the mathematical-physical model of faulting by means of a direct application of the theory of continuum distribution of dislocations. For such a model the displacements at any point in an infinite homogeneous medium are calculated.

The new model first is tested by assuming constant friction on the fault plane, which makes the model similar to all the conventional earthquake models, and then is compared with them. From the comparison a very simple relationship between the total dislocation and the effective stress is found, identical to a relation given by considering a distribution of continuum dislocations only.

Next, the amplitude spectrum is evaluated. It is flat at the low-frequency end where its level is proportional to the effective force acting on the fault plane. However, at the high frequency end, the spectrum shows a roll-off which is inversely proportional to the second power of the frequency. The intersection of the two asymptotes defines a point whose abcissa (corner frequency) is related to the fault area. The effective force and fault area thus obtained give the same expression for the seismic moment as is obtained by the conventional models (Keylis-Borok, 1960; Aki, 1967; Brune, 1970). The equations derived in this study were employed to calculate the source parameters of the San Fernando earthquake, which parameters were then compared to the values of the parameters observed by other studies and the results were comparable, demonstrating that this limiting case of the theory is correct, and that the application of the theory of continuum distribution of dislocations to model earthquake sources is feasible. The theory derived in the present study has the advantage that it enables us to include variable friction on the fault plane, and to study the effect of such variable friction on the radiation of seismic wave energy.

Next, a simple functional dependency of friction with one coordinate was assumed, namely, a linear increase of friction along this one coordinate. As an example, consider the case of an increase in friction with depth due to the increase in hydrostatic stress, where a minimum frictional stress occurs at the top of the fault, and a maximum frictional stress is found at the bottom or end of the fault. In this case a unilateral faulting model was used, with the externally applied stress and the minimum frictional stress at the top of the fault kept constant. The effective stress is different at every point on the fault in the direction of motion, modulating the amplitude of the perturbation. This results in a kind of slip-stick displacement moving at supersonic velocities between two consecutive points that are separated by infinitesimal distances, although the overall slippage is uniform and moving at either supersonic or subsonic velocities. It is clear that the efficiency of radiated waves at any point is dependent on not only the applied stress but also the maximum frictional stress. The displacement for this model was calculated, and it was found that the amplitude and width of the stopping phase increased with an increase in the maximum friction which, as mentioned before, occurs at the end of the fault.

Finally, the amplitude spectrum for this model was calculated. It was found that the high frequency end falls off with the second power of the frequency independently of the applied stress and the maximum frictional stress. The amplitude of the high frequency oscillations depends on the ratio of the maximum frictional stress to the externally applied stress. For values of this ratio less or equal to one, that is for normal or forward slippage, an increase in the maximum frictional stress smooths out the high frequency oscillations. For values of the ratio greater than one but less than two, which apparently corresponds to the case of partial or complete rebound or slip-back, the amplitude of the high frequency oscillations starts to increase again with increasing maximum frictional stress.

The low frequency part of the amplitude spectrum was found to be almost flat, increasing slightly toward the very low frequencies, although it was found to be bounded (finite) at zero frequency. The level of the low frequency amplitude spectrum was also found to be dependent on the ratio of the maximum frictional stress to the externally applied stress. In general the level of the low

frequency portion of the amplitude spectrum decreases with an increase in the maximum frictional stress for values of the ratio less or equal to one. The rate of decrease of the level of the amplitude spectrum at zero frequency is greater than that of the amplitude at somewhat larger, but still low frequencies, for values of the ratio greater than one. This zero-frequency amplitude spectrum level reaches a minimum of zero at a value of the ratio equal to two (complete rebound). For even larger values of the ratio there is an overshooting of the rebound over the normal slippage. If one considers friction to be an absorbing phenomenon, energy considerations give an upper bound of this ratio equal to two. The overall effect of a linear increase of friction is that we have a flat amplitude spectrum for normal slippage similar to the model with constant friction, with its low frequency level depending upon the values of the maximum frictional stress and externally applied stress. The corner frequency is dependent on the geometry and physical parameters of the fault. For the rebound case a predominant peak in the spectrum is found resembling that obtained by Archambeau's elastodynamic spectral model. The frequency of the predominant peak (peak frequency) is dependent on the values of the applied external stress, the maximum frictional stress, and the geometry and velocity of rupture of the fault. All these spectral models are dependent on the time-displacement constant. For small and moderate values of the time-displacement constant all the above conclusions remain unchanged. However, for extremely high values of the time-displacement constant, it was found that the amplitude spectrum increases monotonically toward the low frequencies for normal slippage, although, as before, it is bounded at zero frequency. Backward slippage and extremely high values of the time displacement constant result in an amplitude spectrum with a less pronounced peak.

Next, to see whether, independent of the value of the time-displacement constant, it was possible to get a monotonically increasing amplitude spectrum toward the low frequencies for the case of normal slippage a second-power increase of friction with depth was assumed. It was found, however, that even with a stronger dependency of friction on depth, the low frequency portion of amplitude spectrum is still practically flat for normal slippage. In the case of rebound slippage for values of the ratio of the maximum frictional stress to the externally applied stress somewhat less than two, the most peaked spectrum was obtained.

Next, an anomalously low frictional stress was considered to exist at the point of initiation of the rupture process, physically identified in actual earthquakes with the hypocenter, where presumably the fracture starts. Ground displacement and the amplitude spectrum were calculated for such a model, assuming bilateral faulting. It was found that the final expressions for the displacement and its spectrum were a combination of three terms. One is equal to that of a unilateral fracture growing upwards, contributing always to normal slippage; another is equal to unilateral faulting, with the fracture growing downward toward the end of the fault, giving normal and backward slippage; and the third results from a mixed contribution of the first two. The overall spectrum shape depends on the relative importance of the first two contributions. Yet it was found that the high frequency end remains inversely proportional to the second power of the frequency, and the level of the amplitude spectrum at zero frequency depends upon the depth of the hypocenter, the depth of the bottom end of the fault, and the ratio of the maximum frictional stress at the end of the fault to the applied external stress. For various combinations of these parameters it was found that one could obtain either a flat spectrum or a peaked spectrum with this model. For combinations of these parameters that best approximate nature, the model favors a flat spectrum, whose low frequency level is dependent on the applied stress, the minimum and maximum frictional stress, and whose corner frequency depends on the dimensions and physical parameters of the fault.

Finally, a more realistic model that approximates best what happens in nature was considered. The lowest frictional stress region is assumed to occur at the hypocenter, from which point bilateral fracturing spreads. Frictional stress is assumed to increase from the surface of the earth, due to an increase in the hydrostatic stress, down to some depth. From this depth to the hypocenter friction is assumed to decrease, as might occur in a low-Q zone. From the hypocenter to some greater depth the frictional stress is assumed to increase linearly, and beyond this greater depth to increase even more rapidly. The model is a combination of all the simplified models treated. It was still found that the high frequency roll-off remains inversely proportional to the second power of the frequency. The zero-frequency level of the amplitude spectrum depends especially on 1) the ratio between the largest frictional stress that occurs above the low frictional zone to the applied stress, 2) the ratio between the

maximum frictional stress at the end of the fault to the applied stress, 3) the focal depth, and 4) the depth of the end of the fault. For various combinations of these parameters both flat and peaked spectra were found to occur. Qualitatively the model seems to explain the two kinds of New Madrid earthquake spectral groups observed by digital and analog spectral analysis of 17 events recorded by the St. Louis University network. The model also enables us to calculate fault parameters such as the maximum frictional stress, average stress drop, seismic moment, and effective stress. The actual calculations, however, will be the subject of a separate study.

References:

Keylis-Borok, V. I. (1960). Investigation of the mechanism of earthquakes, Sov. Res. Geophys. (English translat.), 4, 29.

Aki, K. (1967). Scaling law of seismic spectrum. J. Geophys. Res., 72, 1217-1231.

Brune, J.N. (1970). Tectonic stress and spectra of seismic shear waves from earthquakes, J. Geophys. Res., 75, 4997-5009.

III.2 P-wave source spectra from observations of deep-focus earthquakes at small epicentral distances, by Rama Somayajulu.

Seven deep-focus earthquakes (depth greater than 550 km) were studied, to determine the spectrum of their P wave motion near the source from the seismograms of neighboring South American stations. The method developed by Rogers (Appendix II.1) was employed to determine the thickness and dip angle of the crust at the seismograph station from the observed horizontal and vertical component spectra of the P wave motion. Once the crustal thickness and dip of the crust are known, their effects on the observed spectra can be removed, to yield the horizontal and vertical components of the spectrum in the mantle. Because the ray path from the focus to the mantle beneath the station is short, it seems reasonable to assume that the attenuation along the path is small, so that the calculated mantle spectrum approximates the source spectrum.

This procedure of calculating the source spectrum was applied to the data of seven earthquakes, as recorded at four stations. Table 1 contains the dates, location and magnitude of the earthquakes, and the WWSSN stations whose seismograms were used in the study. The locations of the epicenters and stations are shown in Figure 1.

Table 1

Earthquakes and Seismograph Stations Used in Study

| No. | Date | Latitude | Longitude | Origin Time | Depth | $m_b$ | Stations |
|---|---|---|---|---|---|---|---|
| 1 | 11 Nov 1963 | 9.1°S | 71.4°W | $19^h54^m$ | 585 km | 4.9 | NNA |
| 2 | 18 Feb 1965 | 9.9 | 71.2 | 22 32 | 594 | 5.2 | NNA |
| 3 | 22 Dec 1964 | 9.5 | 71.3 | 00 24 | 614 | 5.3 | NNA |
| 4 | 9 Sep 1967 | 27.75 | 63.1 | 10 06 | 578 | 5.8 | NNA |
| 5 | 5 Mar 1965 | 27.04 | 63.3 | 14 32 | 573 | 5.5 | ANT, LPB NNA, PEL |
| 6 | 17 Jan 1967 | 27.45 | 63.3 | 01 07 | 588 | 5.6 | ANT |
| 7 | 23 Aug 1968 | 22.05 | 63.5 | 22 36 | 537 | 5.8 | LPB |

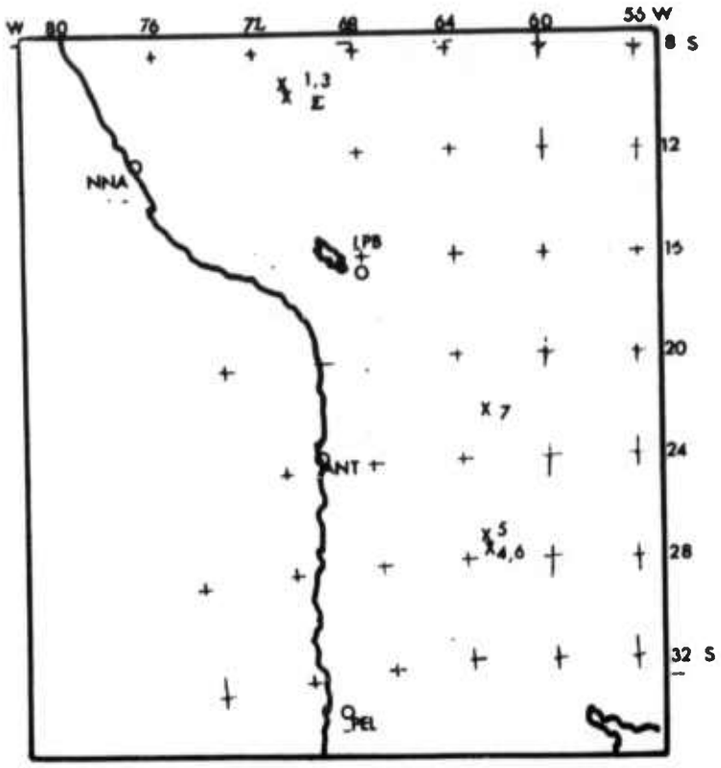


Figure 1. Location of stations and earthquakes used for study. The numbers refer to the earthquakes given in Table 1.

All the mantle P wave spectra were found to decrease as $f^{-2}$ at the high frequencies and to be flat at the low frequencies, with the exception of the two deduced from the ANT data. For the 5 March 1965 earthquake, the mantle spectrum of ANT shows a pronounced peak at about 0.3 Hz. The mantle spectrum deduced from the ANT seismograms for the earthquake of 17 January 1967 also shows a peak, but not so pronounced, at 0.3 Hz.

Figure 2 shows the smoothed vertical component spectra of the mantle P-wave motion as deduced from the data of ANT, LPB, NNA and PEL. The difference in level of the low-frequency part of the LPB spectrum might be explained by the focal mechanism, and the fall-off of the NNA spectrum between frequencies of about 0.08 and 0.4 Hz by greater-than-normal absorption in the frequency band for the hypocenter to station path. However, the peak in the ANT spectrum remains unexplained.

III.3 Calculation of near-field motion for CANNIKIN from far-field data, by Otto W. Nuttli.

Formulas derived by Nuttli (Appendix I.9) will, in theory give hard-rock motion produced by Rayleigh waves in the near-field region for periods greater than 1 sec if $M_S$ is known. The formulas are based upon a point-source model of elastic waves, which seems appropriate for underground explosions. When observations of hard-rock motion for the nuclear explosion CANNIKIN became available (L. R. West and R. K. Christie, Observed Ground Motion Data, Cannikin Event, Environmental Research Corp., Report NVO-1163-230, December, 1971), the author decided to compare the observed data with values calculated from the theory mentioned above. One additional assumption is necessary, namely the shape of the Rayleigh-wave amplitude spectrum in the near-field region. For the purposes of this study, it was assumed to be flat at periods above 5 sec, and to fall off as $f^{-1}$ from periods of 5 to 1 sec.

A value of $M_S = 5.7$ was taken for CANNIKIN, from published reports. This value is an average, based on measurements of the amplitude of 20-sec period waves at teleseismic distances.

Peak particle velocity and peak displacement data were available for eight points at slant distances of 10.4 to 36.5 km, and at points at distances of 305 and 370 km. The periods of the wave motion at which these peak values occurred also are known.

Using $M_S = 5.7$ and the theoretical attenuation curve for 20-sec period surface waves (Nuttli, Appendix I.9), it was found that A at 305 km was 1770 microns

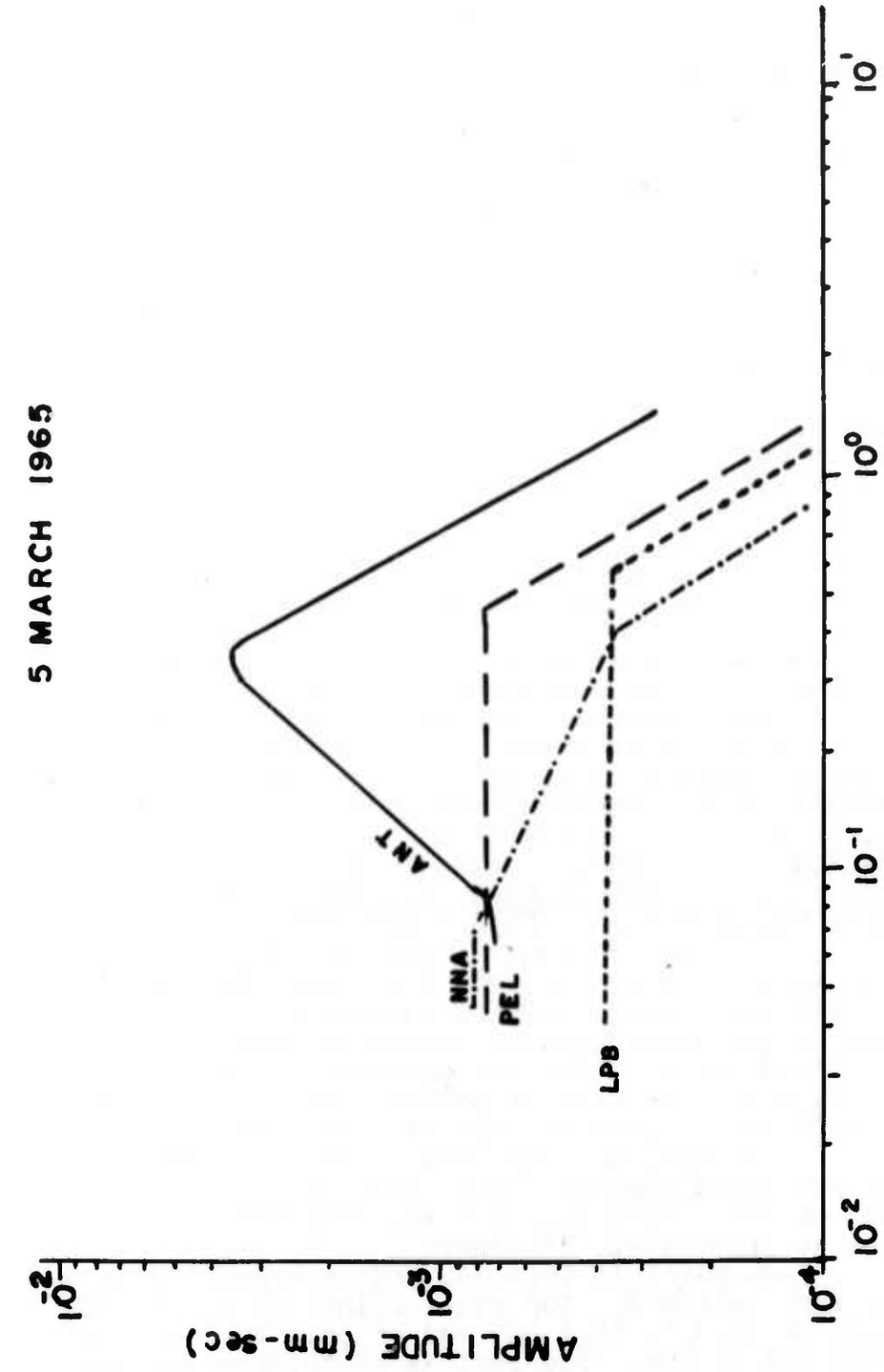


Figure 2. Smoothed P-wave spectra (vertical component of motion) in mantle beneath the seismograph stations, for the earthquake of 5 March 1954.

for 20-sec period curves. Assuming a flat amplitude spectrum from 20 to 5 sec, and a fall-off of $f^{-1}$ from 5 to 1 sec, the value of A at 1.65 sec is 580 microns, and if particle velocity is $2\pi$ (580/1.65) = 2200 microns/sec = 2.20 mm/sec. Similar reasoning applied to the particle velocity at 370 km distance, where the peak value of the vertical component of particle velocity occurred at a period of 1.50 sec, gives A = 445 microns and particle velocity = $2\pi$ (455/1.50) = 1.90 mm/sec. Our assumption of the amplitude spectrum falling off as $f^{-1}$ between 5 and 1 sec implies that the velocity spectrum is flat between these periods.

The maximum amplitude of the vertical component of motion at $\Delta$ = 305 km occurred at a period of 1.80 sec. Extrapolating the 20-sec period motion at teleseismic distances back to 305 km, and assuming the same shape of the near-field spectrum as above, gives a calculated value of 480 microns or 0.58 mm at 1.80 sec period. The calculated displacement at $\Delta$ = 370 km for a period of 2.80 sec is 850 microns or 0.85 mm.

Table 2 compares some observed and calculated values of the near-field motion of CANNIKIN. The calculated and observed values of the maximum displacement and particle velocity agree quite well for $\Delta$ = 305 and $\Delta$ = 370 km, as can be seen from the table. However, at the closer distances of 10, 20 and 36 km the calculated values are always smaller than the observed, sometimes by an order of magnitude. The likely explanation is that the observed peak values at distances of 10 to 36 km result from body-wave motion, which likely is larger than the Rayleigh-wave motion at these small distances. The calculated values of the motion, which are for Rayleigh waves, can therefore be expected to be smaller than the observed values.

It is unfortunate that there are no observations of ground motion at distances between 36 and 305 km. It would be of interest to know the minimum distance at which the Rayleigh wave motion exceeds the body-wave motion, and thus how close-in one could use the formulas in Appendix I.9 to predict near-field peak motion.

III.4 Relation between $M_S$ and $m_b$ for central United States earthquakes, by Otto W. Nuttli.

The body- and surface-wave magnitudes of eight earthquakes that occurred in the central United States were carefully evaluated, to determine the relation between these two magnitudes. The body-wave magnitudes were determined from teleseismic P waves and from $P_n$ waves, in the former case using the standard Gutenberg-Richter calibration curve and in the latter using Evernden's formula for eastern North America. Both formulas give the same $m_b$ value, when there are sufficient teleseismic P-wave amplitude data available.

Table 2

Observed and Calculated Values of Near-Field Motion

of CANNIKIN (Vertical Component of Motion)

| Horizontal Distance | Peak Particle Vel.(Observed) | Peak Particle Vel.(Calculated) | Period of Peak Part.Vel. | Peak Displacement (Observed) | Peak Displ. (Calculated) | Period of Peak Displ. |
|---|---|---|---|---|---|---|
| 10 km | 35.1 cm/sec | - | 0.45 sec | 6.63 cm | 1.8 cm | 3.22 sec |
| 20 | 11.6 | 1.95 cm/sec | 1.22 | 3.45 | 1.1 | 3.15 |
| 36 | 8.5 | 1.23 | 3.02 | 4.42 | 0.35 | 3.15 |
| 305 | 0.224 | 0.22 | 1.65 | 0.0632 | 0.058 | 1.80 |
| 370 | 0.232 | 0.19 | 1.50 | 0.0596 | 0.085 | 2.80 |

Table 3

$m_b$ and $M_S$ Values for Earthquakes in the Central United States

| Date | Latitude | Longitude | Origin Time | $m_b$ | $M_S$ |
|---|---|---|---|---|---|
| 9 November 1968 | 37.9°N | 88.5°W | $17^h01^m42.0^s$ GMT | 5.50 | 5.20 |
| 21 October 1965 | 37.5 | 91.1 | 02 04 39.3 | 4.85 | 4.10 |
| 3 March 1963 | 36.7 | 90.1 | 17 30 13.0 | 4.76 | 4.08 |
| 15 September 1972 | 41.6 | 89.3 | 05 22 15.5 | 4.39 | 3.34 |
| 17 November 1970 | 35.9 | 89.9 | 02 13 54.3 | 4.29 | 3.20 |
| 21 July 1967 | 37.5 | 90.6 | 09 14 48 | 4.21 | 2.84 |
| 1 October 1971 | 35.8 | 90.4 | 18 49 38.7 | 4.14 | 2.65 |
| 14 August 1965 | 37.2 | 89.3 | 13 13 56.6 | 3.81 | 2.54 |

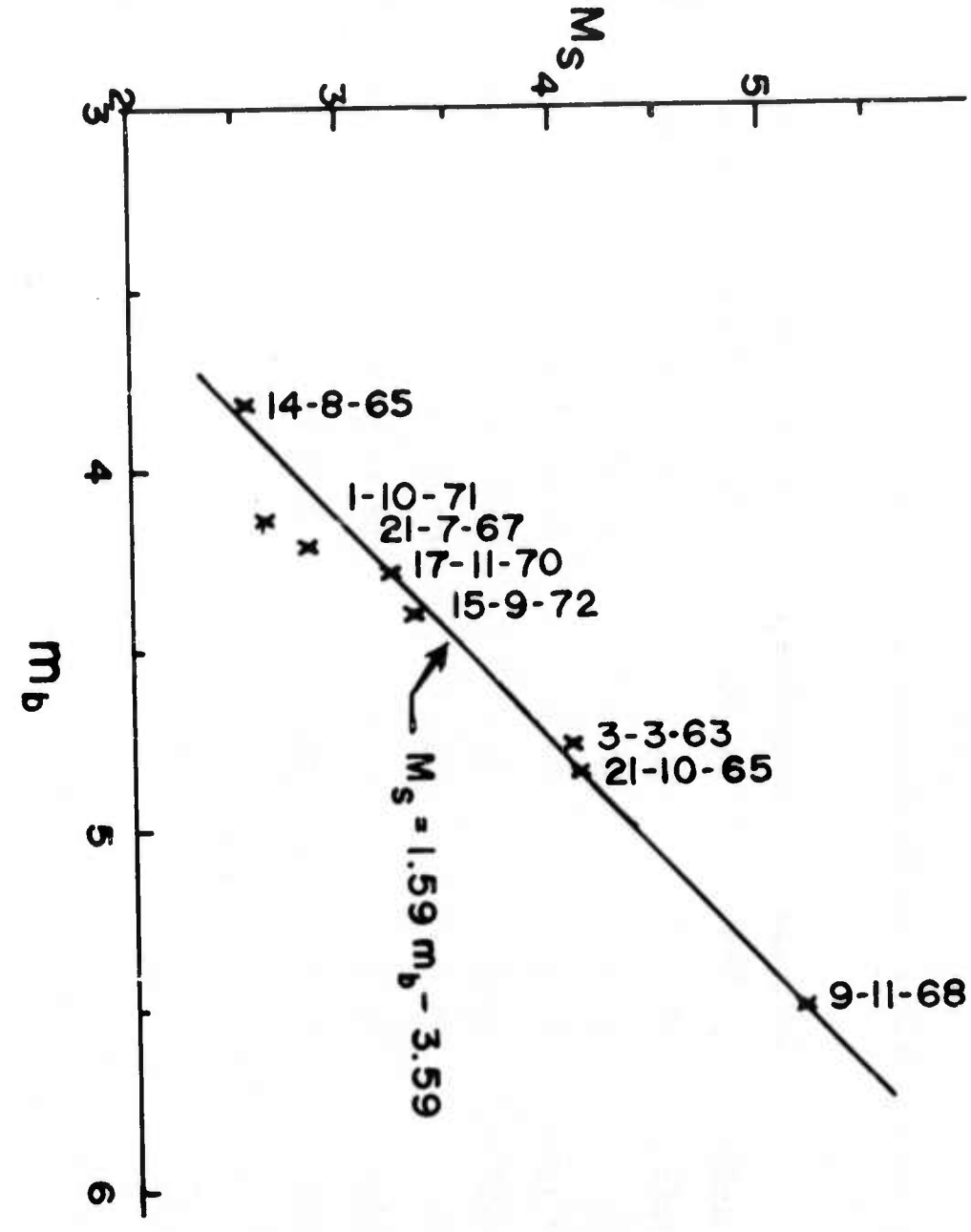


Figure 3. Ms vs mb plot of earthquakes in central United States.

Surface-wave magnitudes were determined from 20-sec period surface wave data at teleseismic distances, and from 3- to 12-sec period Rayleigh waves at closer distances (Nuttli, Appendix I.9). The two methods of determining $M_s$ gave similar values for $M_s$, for those earthquakes for which 20-sec period waves could be observed. For the smaller earthquakes $M_s$ was determined from the 3- to 12-sec period Rayleigh wave amplitudes only, and $m_b$ from the $P_n$ amplitudes only.

The results are summarized in Table 3, and plotted in Figure 3. Data for the magnitude determinations came from the WWSSN and Canadian Network seismograms. From the figure it can be seen that six of the points lie close to the line $M_s = 1.59\ m_b - 3.59$. The two anomalous points correspond to the 1 October 1971 and 21 July 1967 earthquakes. The former was one which Rodriguez and Kisslinger (Appendix I.1) found to be deficient in low-frequency energy. The magnitudes of this earthquake support their finding, because $M_s$ is about 0.4 units too small for the corresponding $m_b$ value.

No spectrum analysis has as yet been done on the seismograms of the 21 July 1967 earthquake, to determine if it also is deficient in low-frequency energy.

The magnitude relation $M_s = 1.59\ m_b - 3.59$ differs by a constant from that found on a world-wide basis by Gutenberg and Richter, namely $M_s = 1.59\ m_b - 3.97$. However, considering that Gutenberg and Richter's formula was derived from data with $M_s$ in the range of about 6 to 8.5, and the formula for the central United States for $M_s$ in the range 2.5 to 5, the similarity between the two formulas is surprising.

III.5 Study of seismic shear waves and upper mantle structure in the western United States, by Tuncay Yasar.

The western United States is marked by an upper mantle of abnormally low seismic velocities, high seismic wave attenuation and high heat flow relative to other continental areas. Both P and S arrivals are systematically late with respect to those in the central and eastern United States. These late arrivals and other geophysical observations have shown that a low velocity channel exists in the western United States.

Arrival times of short- and long-period P waves and of long-period S waves were read from 35 earthquakes at stations ALQ, DUG, GOL, LUB, GSC, TUC, BKS, BOZ, COR, LON, RCD, FLO of the World Wide Standard Stations (WWSS) network and DRCO, HLID, KNUT, LCNM, LGAZ, MNNV,

NLAZ of the Long Range Seismic Measurements (LRSM) network. Absolute residuals at each station were obtained by using the Jeffreys-Bullen Tables. To reduce the source effect and that of errors in the travel-time tables, residuals were subtracted from the residuals at one station, ALQ. These are called S residuals.

The S residuals are interpreted on the assumption that they result from lateral variations in thickness of the shear-wave low-velocity channel in the western United States. The depth to the top of this channel is found to decrease rapidly in going inward from the coast, with the top of the channel approaching the M-discontinuity in southeast Nevada, northwest Arizona and southwest Utah.